A New Multilevel Z-Source Inverter for Distributed Generation

T.Sripal Reddy
Associate professor & HoD
Department of Electrical &
Electronics Engineering,
Sarada Institute of Technology &
science,
Khammam, Telangana, India.

A.Rajababu
Assistant Professor
Department of Electrical &
Electronics Engineering,
Sarada Instituteof Technology &
science,
Khammam, Telangana, India.

P. Ravindra
M.Tech Student
Department of Electrical &
Electronics Engineering,
Sarada Instituteof Technology &
science,
Khammam, Telangana, India.

ABSTRACT

Distributed generation is an emerging concept in the electricity sector, which represents good alternatives for electricity supply instead of the traditional centralized power generation concept. Distributed generation represents a small-scale electric power source connected directly to the utility's distribution network and provides electric power at a site closer to the customer, rather than through lengthy transmission lines spanning from central power stations. When it is fully implemented, can provide reliable, high quality and low-cost electric power the different schemes that are available for distributed generation are solar energy, wind energy, micro-turbines and fuel cells. In this context, the impedance-source (Z-source) inverter based topologies provide a modern approach to the step-up voltage conversion techniques. The main feature of the Z-source inverter is that it can boost the input voltage by introducing a shoot-through operation mode. It means the simultaneous conduction of both the switches of the same phase leg of the inverter, which is forbidden in traditional voltage source inverter. This paper further addresses detailed modeling and control issues of the quasi ZSI used for distributed generation (DG), such as PV or fuel cell power conditioning. The dynamical characteristics of the quasi ZSI network are first investigated by small-signal analysis. Based on the dynamic model, stand-alone operation and grid-connected operation with closed-loop control methods are carried out, which are the two necessary operation modes of DG in distributed power grids. In extension to the work the inverter is replaced with five level Neutral point clamped Multilevel Inverter which has the advantages of low dv/dt, less EMI, and low THD. The proposed converter tested by using Matlab/simulink software.

Index Terms—DC–AC converter, distributed generation (DG), quasi-Z-source inverter (q-ZSI), renewable energy source (RES).

I.INTRODUCTION

Photovoltaic (PV) power generation is becoming more promising since the introduction of the thin film PV technologydue to its lower cost, excellent high temperature performance, low weight, flexibility, and glass-free easy installation [1]. However, there are still two primary factors limiting the widespread application of PV power systems. The first isthe cost of the solar cell/module and the interface converter system; the second is the variability of the output of the PVcells. A PV cell's voltage varies widely with temperature and irradiation, but the traditional voltage source inverter(VSI) cannot deal with this wide range without over rating of the inverter, because the VSI is a buck converter whoseinput dc voltage must be greater than the peak ac output voltage [2]-[3]. A transformer and a dc/dc converter is usuallyused in PV applications, in order to cope with the range of the PV voltage , reduce inverter ratings, and produce adesired voltage for the load or connection to the utility.In Recent Years, wind energy has been regarded as one of the significant renewable energy sources [4]. Among theexisting wind power generation systems, their generators can be categorized into four main types: 1) fixed-speedsquirrel-cage induction generator, 2) variable-speed wound rotor induction generator that employs variable rotorresistance, 3) variable-speed doubly fed induction generator that employs a frequency converter between the grid andits rotor windings and 4) variable-speed synchronous generator,

which is either a wound rotor synchronous generator or a permanent-magnet synchronous generator (PMSG). Due to the fact that a multiple pole design can be easily realizedin the synchronous generator, it is the only type that provides a realistic opportunity to implement gearless operationand hence, the features of lightweight and low maintenance can be obtained in wind generation system [5]-[6].

The Z-source inverter (ZSI) has been reported suitable for residential PV system because of the capability of voltage boost and inversion in a single stage. Recently, four new topologies, the quasi-Z-source inverters (q-ZSI), have been derived from the original ZSI. This paper analyzes one voltage fed topology of these four in detail and applies it to PV power generation systems. By using the new quasi Z-source topology, the inverter draws a constant current from the PV array and is capable of handling a wide input voltage range. It also features lower component ratings and reduced source stress compared to the traditional ZSI.
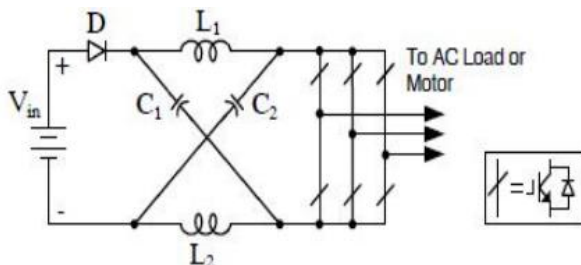
Fig.1. Voltage fed Z-source inverter
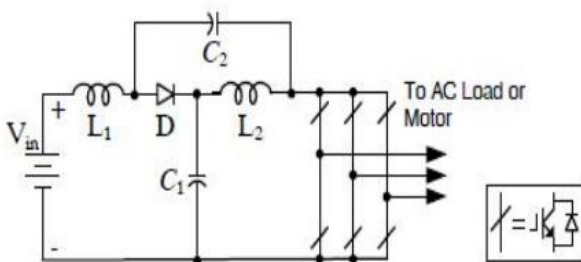
Fig.2. Voltage fed quasi-Z-source inverter

Figs. 1 and 2 shows the traditional voltage fed ZSI and the proposed voltage fed QZSIrespectively. In the same manneras the traditional ZSI, the QZSIhas two types of operational states at the dc side, the nonshoot-through states (i.e. thesix active states and two conventional zero states of the traditional VSI) and the

shoot-through state (i.e. both switchesin at least one phase conduct simultaneously).Fig. 3 shows the proposed QZSIin the PV power generation system. It connects the PV arrays and outputs three phase 50 Hz, 330 V ac to resistive loads, which is the standard utility level. A three-phase LC Filter connected in right after the inverter bridge to get 50Hz sinusoidal ac outputs.
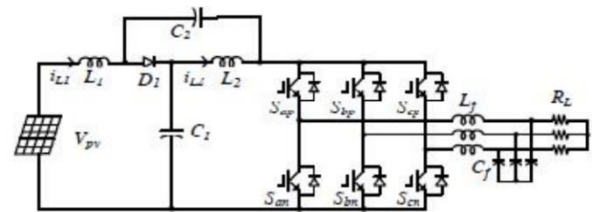
Fig.3. QZSI in the PV power generation system

II. DYNAMICMODELING OF THE QUASI-Z-SOURCENETWORK
A. Small-Signal Model of the Quasi-Z-Source Network

By applying a two-stage control strategy to be presented later on, the control of dc side and that of ac side are decoupled. With an intention to provide a comprehensive mathematical guide in terms of the QZSI dc-side modeling, small-signal analysis is used for the studies, along with detailed derivations. For general analysis purposes, input voltage v_{in} is chosen as system input, to which input current I_{in} is related. This is because RES does not have as stiff output characteristics as an ideal voltage source or current source. The relationship of V_{in} and I_{in} will be determined by specified energy source nature. For dc-side modeling, the three-phase inverter bridge and external ac load are represented by a single switch and a current source connected in parallel [17], [19].Considering the asymmetric quasi-Z-source network, there are four state variables: the currents through two inductors$i_{L1}$and i_{L2} and the voltages across the capacitors v_{C1}andv_{C2}. Independent load current i_{load} serves as another input (disturbance) of the quasi-Z-source network. Choose v_{C1} and $i_{L1}(=i_{in})$as the output of the studied system. For simplification, assume that $C=C_1=C_2$,$L=L_1=L_2$, the stray resistances of inductors $r=r_1=r_2$, and the equivalent series resistances of capacitors $R=R_1=R_2$. Define shoot-through interval T_0, non-shoot through interval T_1, and switching

period $T_s=T_0+T_1$; thus, the shoot-through duty ratio isd0=T_0/T_s. At the shoot-through state the capacitors transfer their electrostatic energy to magnetic energy stored in the inductors. The dynamic state equations of the quasi-Z-source network are given as

$$\frac{dx}{dt} = A_1 x + B_1 u$$

At the non-shoot-through states the dc power source, as well as the inductors, charges the capacitors and powers the external ac load, boosting the dc voltage across the inverter bridge. The dynamic state equations are shown as

$$\frac{dx}{dt} = A_2 x + B_2 u$$

Using state-space averaging, the dc-side model of Q-ZSI can be obtained as shown in

$$\frac{dx}{dt} = Ax + Bu \qquad y = Cx + Du$$

To obtain the small-signal model, perturbations $\hat{d}_0$, $\hat{v}_{in}$, and $\hat{i}_{load}$ are introduced with d0, vin, and iload, respectively, which, in turn, cause variations $\hat{i}_{l1}$, $\hat{i}_{l2}$, $\hat{v}_{c1}$, and $\hat{v}_{c2}$ in the dynamic state variables of iL1, iL2, vC1, and vC2. Substituting x=X+$\hat{x}$ (where X and $\hat{x}$ are the dc terms and perturbations of the variables x=d0, vin, iload, iL1, iL2, vC1, and vC2) into (3), considering the principles of inductor volt–second and capacitor charge balance in steady state and ignoring the second-order elements, the Laplace-transformed transfer functions of the multi-input multi output quasi-Z-source network can be derived.
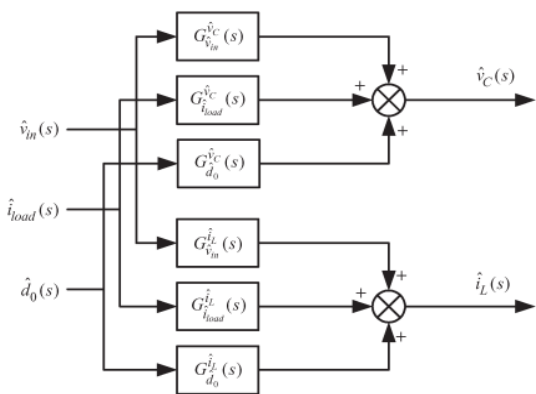
Fig.4. Small-signal model of the quasi-Z-source network.

The small-signal model of the quasi-Z-source network is shown in Fig.4. Assuming any two of the system inputs to be zero, one can get small-signal transfer functions from the remaining to the state variables.

B. Dynamic Characteristics of the Quasi-Z-Source Network

According to the small-signal model, the transfer functions from d0 to capacitor voltages vC1 and vC2 are identical, denoted as $G_{d_0}^{\hat{v}_c}(s)$ in (4), shown at the bottom of the page. Other transfer functions are given in the Appendix. Based on these equations, the characteristic equation of the quasi-Z-source network can be obtained as

$$s^2 + \frac{r+R}{L}s + \frac{(1-2D_0)^2}{LC} = 0$$

Equation (5) can be written as the following normalized form:

$$s^2 + 2\xi\omega_n s + \omega_n{}^2 = 0$$

Where

$$\omega_n = \frac{1-2D_0}{\sqrt{LC}}$$

is the natural frequency a

$$\xi = \frac{r+R}{2(1-2D_0)}\sqrt{\frac{C}{L}}$$

is the damping ratio. Among these equations, D_0, I_{load}, V_{C1}, V_{C2}, I_{L1}, and I_{L2} represent a given equilibrium point nearby where the system can be linear zed. Equation (5) indicates that, aside from the parameters of the quasi-Z-source network (i.e., L, C, r, and R), D_0 is also one factor to determine the system dynamic characteristics. To make a clear map of the dynamic characteristics of the quasi-Z-source network, various root loci of the transfer function $G_{d_0}^{\hat{v}_c}(s)$ are studied by parameter sweep of L, C, and D_0. The system specifications are as follows: L= 500μH, C= 400μF, R=0.03 Ω, r=0.47 Ω, D0=0.25, Iload=9.9A, and Vin = 130V. Fig. 5 shows the pole and zero trajectories of $G_{d_0}^{\hat{v}_c}(s)$ with L, C, and D_0 variations, respectively. The quasi-Z-source network exhibits similar characteristics as the Z-source network studied

in [17]–[19]. There is a right-half plane (RHP) zero in $G_{d_0}^{\hat{v}_c}(s)$ which is learned to imply high gain instability and impose control limitations.
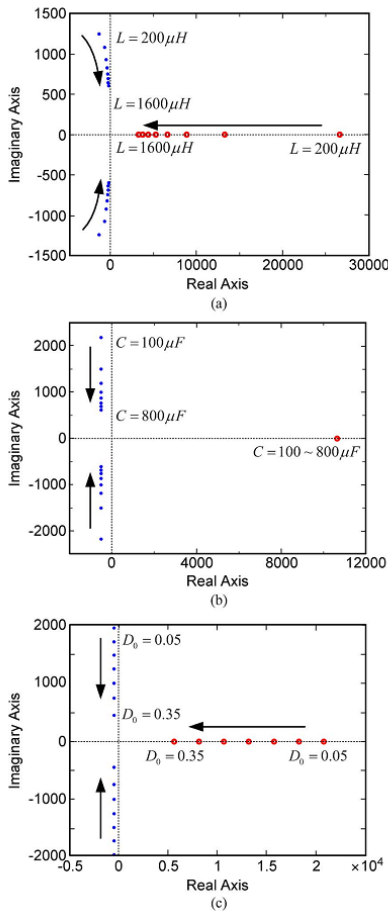
Fig.5. Pole–zero map of transfer function $G_{d_0}^{\hat{v}_c}(s)$ with parameter sweep of (a)L,(b)C,and(c)D0.

A feedback should be carefully designed with an adequate phase margin. It can be observed from Fig. 5(a) that, along with increasing L, zeros are pushed from the right half-plane toward the origin along the real axis, indicating an increasing degree of non minimum-phase undershoot (e.g., capacitor voltage dips before it rises in response to d_0 rising). Similar conclusion can be reached with an increase in D_0 from Fig. 5(c). However, the variation of C has very little influences on the RHP zeros seen from Fig. 5(b). Additionally, the conjugated pole pairs are observed to move toward the origin along with the increase in L, as shown in Fig. 5(a). The feedback control performance is predicted deteriorated with the increase in L. Moreover, increasing in L causes smaller damping

ratio and decreasing natural frequency, which is consistent with (6). On the other side, the conjugated pole pairs can be seen shifting toward the real axis with the increase in D_0orC, implying increasing system settling time and decreasing natural frequency, which is consistent with (6) too. The placement of poles and zeros gives an important guideline for passive component selection of Q-ZSI design: Although large L and C are preferred for low steady-state current and voltage ripples, tradeoffs need to be made for proper transient responses.

III. CAPACITORVOLTAGECONTROL

It is learned from literatures that, to increase voltage gain of the Q-ZSI, one can increase either the shoot-through duty ratio d0 or the modulation index M. However, due to its single-stage structure, d0 and M are dependent on each other. This can be explained by that the voltage boost of Q-ZSI is achieved by partly or fully replacing conventional zero states (000 or 111) with shoot-through state, leaving sixactive states unchangeable [1] (which is associated with M). Thus, (7), (8), or (9) has to be yielded according to the boost method engaged [1]–[3].

Simple boost:

$$M \leq (1 - D_0)$$

Maximum constant boost:

$$M \leq \frac{2}{\sqrt{3}}(1 - D_0)$$

For DG applications, the Q-ZSI is expected to be able to work in both stand-alone and grid-connected modes. To operate in stand-alone mode, DGs in parallel usually construct the distributed power grid in a master–slave manner or all serve as virtual synchronous generators. Thus, the master Q-ZSI or all Q-ZSIs in parallel need to follow a voltage reference to maintain local power balance and valid system voltage and frequency. To operate in grid-connected mode or serve as the slave DG in stand-alone mode, since the output voltage is arbitrarily given by the utility or master DG, the Q-ZSI should follow a current reference to control the output active

and reactive power. To an end, the controlled Q-ZSI turns out two essentially different output characteristics: a voltage source or a current source. The next section will discuss the controller design for both types, respectively. Transition between the two operating modes for DG applications can be made on the micro grid level, where power rebalance and resynchronization are the most concerned aspects. With system reconfiguration by break actions and necessary protections, q-ZSIs can make transition between
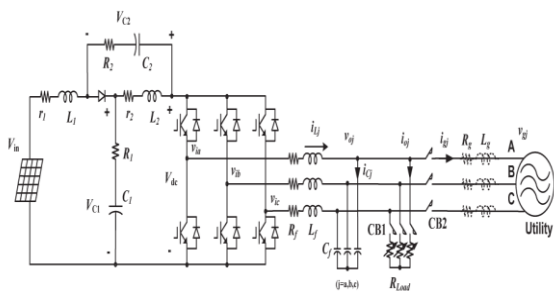
Fig.6. System Configuration of the Proposed Q-ZSI for DG Applications.

Voltage control and current control with precise output power management, relying on modern communication approaches, such as power line or wireless communication.

IV.TWO-STAGECONTROLMETHODOLOGY FOR QZSI-BASEDDG

Fig.6 shows the overall system configuration of the proposed Q-ZSI, where L_f, R_f, and C_f are the inductance, capacitance, and stray resistance of the filter, respectively, and $v_{oj}, i_{Cj}, v_{ij}, i_{Lj}, i_{oj}$, and i_gj are the load voltage, capacitor current of the filter, output voltage of the inverter, inductor current of the filter, load current, and grid current, respectively, all in three phases(j=a, b, c). C_B stands for circuit breaker. C_{B1} is ON and C_{B2} is OFF when the Q-ZSI works under voltage control mode and C_{B1} is OFF and C_{B2} is ON when the Q-ZSI is under current control mode. It should be pointed out that, although one q-ZSI with variable resistive load is used to demonstrate the voltage control strategy, the controller design principle is still applicable to Q-ZSIs that are connected in parallel.

A. Controller Design for Output Voltage Control

Through the decoupling capacitor, control of dc side and that of ac side are executed separately, as shown in Fig.7. Pulses generated by the dc-side controller (for voltage boost) and the ac-side controller (for dc–ac conversion) are combined together by logical OR to fire six insulated-gate bipolar transistors, assuming "1" is ON and "0" is OFF. The overlap of d0 and M can be avoided by setting thereference of the capacitor voltage v∗C_1 based on (13)–(15), depending on the different boost control methods involved. For the dc-side control, capacitor voltage v_{C1} is measured and fed back. The dynamics of v_{C1} caused by d_0 can be obtained via transfer function $G_{d_0}^{\hat{v}_c}$(s),as shown in (4). Linear approximation of the RES output characteristics can be accomplished by the small-signal modeling. Taking PV application as an example, a normal operation for voltage control generally starts from the open-circuit voltage of PV panels Voc and stays at operating points where VPV>VMPP, where VMPP is the voltage at the maximum power point (MPP). Based on the
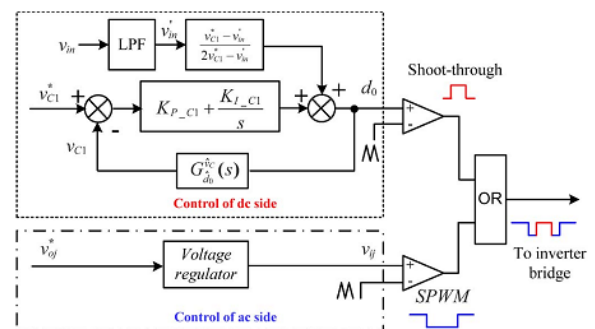
Fig.7. Two-stage control method of the q-ZSI for output voltage control.

Linear approximation, a proportional–integral (PI) controller assisted with a feed forward d_0 is used as the shoot-through compensator. The feed forward d_0 is determined according to the inherent relationship of v_{C1} and v'$_{in}$ in steady state

$$d_0 = \frac{v_{C1}^* - v_{in}'}{2v_{C1}^* - v_{in}'}$$

Where v'$_{in}$ is the input voltage v_{in} after a low-pass filter. Based on the small-signal modeling, PI parameters for the v_{C1}control loop can be decided. In

order to prevent the clashes between the dynamics of ac and dc sides, the dc-side dynamics should be made considerably slower. This could be supported by having a relatively lower bandwidth in the dc-side voltage loop. According to the Q-ZSI network specification in Section II (L=500µH,C= 400µF,R=0.03 Ω, r=0.47 Ω, D0=0.25,Iload =9.9A, and Vin = 130V), the crossover frequencies of the PI controller and low-pass filter are both set to 25 Hz, where KP_C1=1×10−4 and KI_C1=0.8. For the ac-side control, traditional methods explored for voltage regulation are applicable to the Q-ZSI. In a three-phase system, fundamental frequency components are commonly transformed to dc components via d−q transformation, where a simple PI compensator can be applied with good performance. Another choice is to design the controller in stationary frame. Without d−q transformation, the designed controller is applicable to single-phase system too. This paper employs a typical multi loop controller in stationary frame as the voltage regulator,
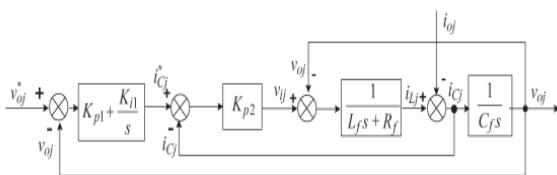
Fig8. Control block diagram of the voltage regulator for Q-ZSI.
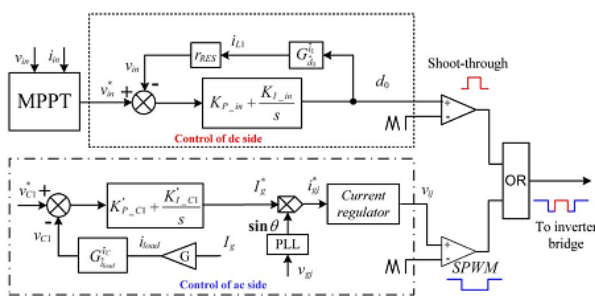
Fig. 9. Two-stage control method for grid-connected-q-ZSI-based PV powerconditioning system.

As shown in Fig.8. From Mason's gain rule, the closed-loop transfer functions can be obtained based on which the ac-side controller can be designed properly. In this implementation, K_{p2} was selected based on the principle of keeping the closed loop gain 0 dB from system output frequency (60 Hz) to half of

the switching frequency (5 kHz in this implementation), where K_{p2}=30. Considering the time delay e−sT s caused by the digital implementation, K_{p2} would be less in practice to maintain a sufficient phase margin for stable performance. The outer voltage loop control parameters K_{p1} and K_{i1} are selected with the compromise that the crossover frequency is low enough to remove the switching harmonics but a sufficiently high bandwidth is retained to have fast response and perfect reference tracking. In this implementation, $K_{p1}$is 0.05 and K_{i1} is 300, where the crossover frequency is 200 Hz and the phase margin is 70◦.

B. Controller Design for Output Current Control

Fig.9 shows the overall diagram of the two-stage control method in grid-connected Q-ZSI, where pulses from control of dc side and that of ac side are combined in the same manner as in the output voltage control mode. For the ac-side control, capacitor voltage v_{C1} is measured and fed back. The magnitude of the grid current reference I^*_g is generated through a PI compensator according to the error signal of v_{C1}. In the case that v^*_{C1}−v_{C1} is positive, power injected into the grid should be reduced to maintain a constant v_{C1}, so negative PI parameters are used here. Along with the phase angle of the grid voltage given by phase-locked loop, the reference of ac current injected into the grid i^*_{gj} can be obtained. Since grid current magnitude is proportional to the equivalent load current i_{load} in small-signal mode, a coefficient G is used to transfer I_g to i_{load}, which relates to inverter operating condition (e.g., modulation index, shoot-through duty ratio, and the power factor). Consequently, the dynamics of v_{C1}caused by load change can be obtained via transfer function $G_{i_{load}}^{\hat{v}_c}$(s),
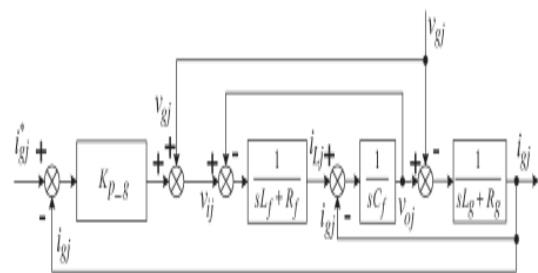
Fig 10 Control block diagram for output current of q-ZSI.

As shown in the Appendix. Similar to voltage control mode,V^*_{C1}should be selected according to (13)–(15), depending on the specific boost control method engaged. Various control methods for the grid-connected inverter can be applied as the current regulator. This project employs a conventional method in stationary frame, which is applicable to single-phase system too. It needs to be noticed that, for the proposed three-phase three-wire system, only two controllers are necessary since the third current is given by the Kirchhoff current law. Fig. 10 shows the block diagram of the current regulator, where a current feedback loop, along with grid voltage feed forward, is used. To an end, parameters of PI compensators for the v_{C1}control loop and vin control loop are chosen based on the following principles: The bandwidth of the v_{in} control loop is lower than that of thev_{C1}control loop, and both of them are lower than that of the current control loop, where K'_{P_C1}=−0.1, K'_{I_C1}= −20, K_{P_in}=−0.002, and K_{I_in}=−0.04 practically. It should be pointed out that, unlike the output voltage control, a valid operating point in output current control can be located on both sides of VMPP. This is because$d_0$is adjusted to track V_{in} in the output current control case, instead of regulating $v_{C1}$for output voltage control. Therefore, MPPT algorithm that sets operating points backward and forward around the MPP can be applied effectively.

V.MATLAB/SIMULINK RESULTS
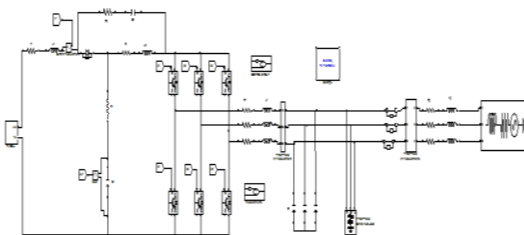
Fig.11 shows the Matlab/simulink model of CCM QZSI topology
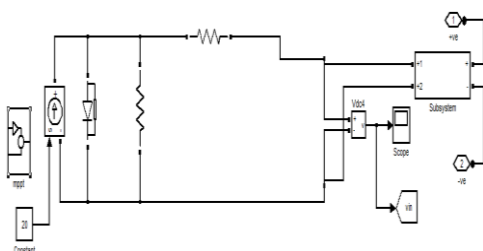
Fig.12 shows the Matlab/simulink model of PV system

Fig.13 output voltage waveform of PV system
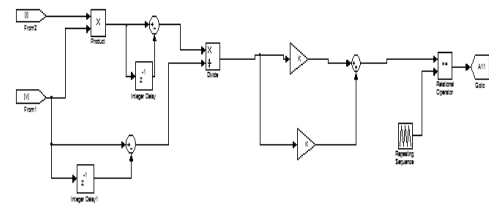
Fig.14 simulink model of MPPT
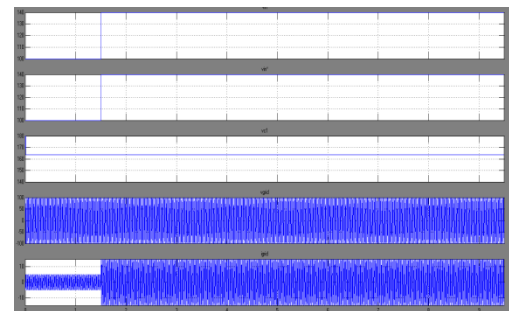
Fig.15 Simulation waveforms of the process of MPPT in the grid-connected QZSI at current controlled mode
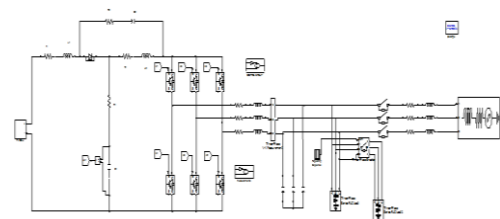
Fig.16 shows the Matlab/simulink model of VCM QZSI topology
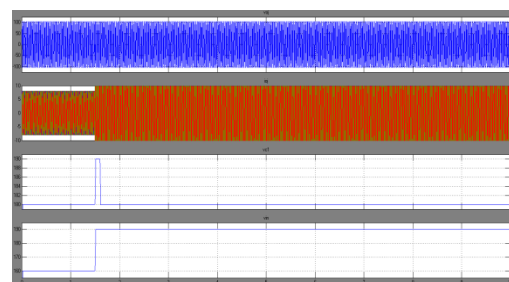
Fig.17 Simulation waveforms of the process of MPPT in the grid-connected QZSI at increasing voltage controlled mode
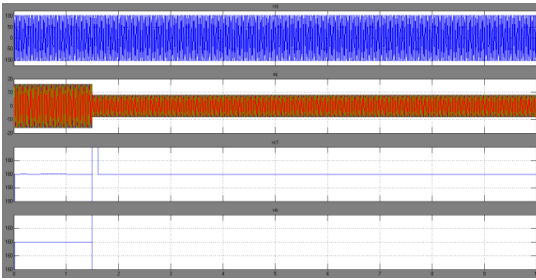
Fig.18 Simulation waveforms of the process of MPPT in the grid-connected QZSI at decreasing voltage controlled mode
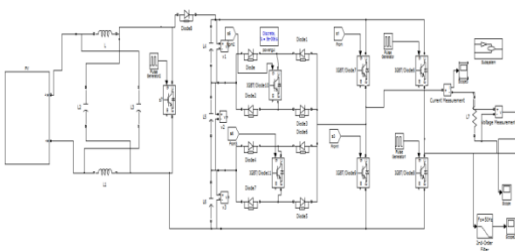
Fig.19 Matlab/simulink model of proposed converter with PWM technique
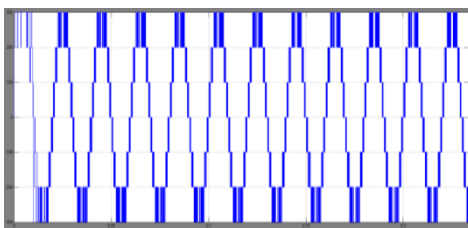
Fig.20 seven level inverter output
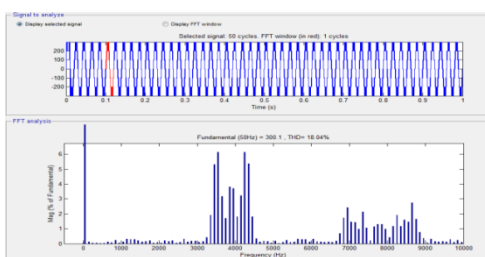
Fig.21 FFT analysis of proposed converter without filter is 18.04%
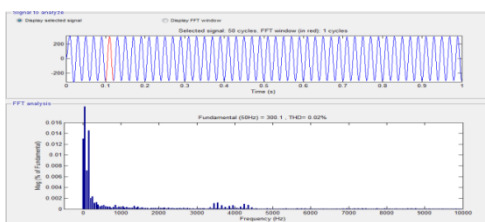
Fig.21 FFT analysis of proposed converter with filter is 0.02%

VI.CONCLUSION

The main aim of this concept to reduce the THD value of the proposed converter by using the filter without filter18.04% by using filter get the 0.02%. In this paper implementation of seven level PWM technique for the proposed QZSI topology converter and emphasized a two-stage control method forthe qZSI-based DG. The dynamical characteristics of the QZSI networkhave been investigated through small-signal analysis.Based on the dynamical model, the two-stage control methodfor QZSI operating in both output voltage control and currentcontrol modes has been presented. MPPT in grid-connectedQZSI-based DG is implemented by the proposed controller.The only drawback of capacitor voltage control approach is that thevoltage stress on devices is unapparent. The all simulation results are verified through Matlab/simulink software.

REFERENCES

[1] F. Z. Peng, "Z-source inverter," IEEE Trans. Ind. Appl., vol. 39, no. 2,pp. 504–510, Mar./Apr. 2003.

[2] F. Z. Peng, M. Shen, and Z. Qian, "Maximum boost control of theZ-source inverter,"IEEE Trans. Power Electron., vol. 20, no. 4, pp. 833–838, Jul./Aug. 2005.

[3] M. S. Shen, J. Wang, A. Joseph, F. Z. Peng, L. M. Tolbert, andD. J. Adams, "Constant boost control of the Z-source inverter to minimizecurrent ripple and voltage stress,"IEEE Trans. Ind. Appl., vol. 42, no. 3,pp. 770–778, May/Jun. 2006.

[4] W. Xiao, N. Ozog, and W. G. Dunford, "Topology study of photovoltaicinterface for maximum power point tracking,"IEEE Trans. Ind. Electron.,vol. 54, no. 3, pp. 1696–1704, Jun. 2007.

[5] W. Li and X. He, "Review of nonisolated high-step-up DC/DC convertersin photovoltaic grid-connected applications,"IEEE Trans. Ind. Electron.,vol. 58, no. 4, pp. 1239–1250, Apr. 2011.

[6] J. M. Carrasco, L. G. Franquelo, J. T. Bialasiewicz, E. Galvan,R. C. P. Guisado, M. A. M. Prats, J. I. Leon,

and N. Moreno-Alfonso,"Power-electronic systems for the grid integration of renewable energysources: A survey,"IEEE Trans. Ind. Electron., vol. 53, no. 4, pp. 1002–1016, Aug. 2006.

[7] C. J. Gajanayake, D. M. Vilathgamuwa, and P. C. Loh, "Development ofa comprehensive model and a multiloop controller for Z-source inverterDG systems,"IEEE Trans. Ind. Electron., vol. 54, no. 4, pp. 2352–2359,Aug. 2007.

[8] Z. J. Zhou, X. Zhang, P. Xu, and W. X. Shen, "Single-phase uninterruptible power supply based on Z-source inverter,"IEEE Trans. Ind. Electron.,vol. 55, no. 8, pp. 2997–3003, Aug. 2008.

[9] F. Z. Peng, M. S. Shen, and K. Holland, "Application of Z-source inverterfor traction drive of fuel cell-battery hybrid electric vehicles,"IEEE Trans.Power Electron., vol. 22, no. 3, pp. 1054–1061, May 2007.

[10] Y. Huang, M. S. Shen, F. Z. Peng, and J. Wang, "Z-source inverter forresidential photovoltaic systems,"IEEE Trans. Power Electron., vol. 21,no. 6, pp. 1776–1782, Nov. 2006.

[11] F. Bradaschia, M. C. Cavalcanti, P. E. P. Ferraz, F. A. S. Neves,E. C. dos Santos, Jr., and J. H. G. M. da Silva, "Modulation for three-phase transformerless Z-source inverter to reduce leakage currentsin photovoltaic systems," IEEE Trans. Ind. Electron., vol. 58, no. 12,pp. 5385–5395, Dec. 2011.